

X-BAND HIGH POWER DRY LOAD FOR NLCTA *

K. Ko, H. Hoag, T. Lee and S. Tantawi

Stanford Linear Accelerator Center, Stanford University, Stanford, CA 94309

Abstract

The specifications for the RF load to be used for absorbing the traveling wave at the end of an NLCTA accelerator section are that it be well matched over a broad band of frequencies (10% minimum), centered at 11.424 GHz, and capable of handling up to 63 MW peak and 3 kW average power. We present a ceramic (Aluminum Nitride + 7% glassy carbon) load design which satisfies these requirements. It consists of a thin strip of dielectric material with a tapered surface placed inside each narrow wall of the waveguide. The complex dielectric constant of the ceramic at X-Band frequencies was first determined by measurement. Based on the measured values, a MAFIA model is used to evaluate the matching and the power dissipation. Results of the simulations indicate an optimal thickness of 0.045 in and overall length of 10in.

I. INTRODUCTION

The NLCTA requires RF loads to absorb the considerable amount of residual traveling wave power exiting each accelerator section. Very compact, high-power water loads have been developed at X-Band frequencies [1]. These are pill-box windows with water circulating on the air side of the ceramic disk to dissipate the power absorbed. They would be suitable for the present application except that there is a potential danger of water leaking into the accelerator section. That occurs when the braze joint between the ceramic disk and the sleeve fails, or if the ceramic disk cracks under high power due to excessive stress. Therefore it is much preferable to have a dry load in which there is no circulating water in direct contact with critical vacuum joints so that this failure mode is eliminated.

We present here one such dry load design. Fig. 1 shows the right top quarter of the geometry looking into the load. It consists of a short section of WR90 rectangular waveguide into which we braze a wedge of lossy ceramic alongside each narrow wall, and on the outside of which we put water cooling channels. The ceramic material is aluminum nitride AlN loaded with 7% glassy carbon which has been used in HOM loads at CEBAF [2] in a lower frequency range, and at much more moderate power levels.

II. LOAD SPECIFICATIONS

The proposed peak RF input power into each 1.8 m section of the NLCTA is 360 MW. The power exiting the end of the section is estimated to be 35% of the input value, or 126 MW. This exiting power is split into two output waveguides and absorbed by the RF loads. The specifications for each of the loads are given in Table 1. Because of the high average power, the



Figure 1. MAFIA 1/4 model of the high-power load.

important issue in the load design is its power-handling capability. It is necessary for the peak dissipated power density in the ceramic to be reasonably low so as not to cause excessive temperature rise and outgassing. This requires the load to be able to spread the power dissipation over a sufficient length. The electric field associated with 63 MW of peak power is not a concern for such a device because the ceramic wedges, being relatively thin and close to the guide sidewalls, are not in a region of high field strength. Since there are no resonant elements, the bandwidth requirement for matching does not pose a problem either. The ceramic properties at X-Band frequencies, however, need to be characterized before any serious design effort can proceed.

Table I
Specifications for NLCTA high-power load.

Peak power	63 MW
Average power	2.84 kW
Center frequency	11.424 GHz
Bandwidth	10 % min.

III. CERAMIC PROPERTIES AT X-BAND

We have determined the complex dielectric constant (ϵ_r, ϵ_i) of the AlN ceramic by measurements and analytical calculations. The experimental setup consists of a .38 in section of WR90 waveguide connected to a network analyzer by a coax-to-waveguide transition. The waveguide was first shorted at the end and the S_{11} in amplitude and phase was measured from 11 to 11.9 GHz. Then a .0615 in thick layer of AlN was fitted over the short and the measurement was repeated over the same frequency range. Since the ceramic comes in batches and its properties may vary from batch to batch, we performed measurements on samples from three different batches. Knowing the level of variability allows for a margin of safety to be incorporated into the design.

From the measured data, we can find the change in the propagation constant β due to the ceramic and with the known geometry, we can calculate the complex ϵ that corresponds to that

*Work supported by the Department of Energy, contract DE-AC03-76SF00515.

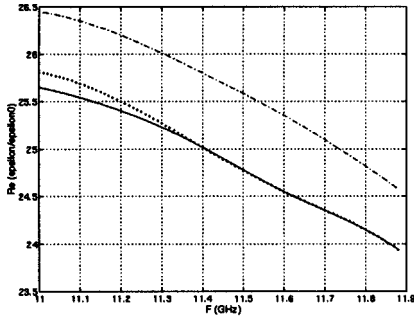


Figure 2. Real part ϵ_r of AlN versus frequency.

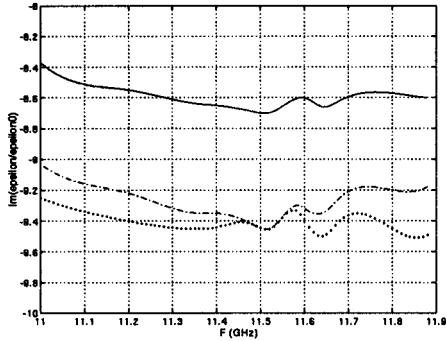


Figure 3. Imaginary part ϵ_i of AlN versus frequency.

change. The results for the three samples are shown in Fig. 2 which refers to the real part ϵ_r , while Fig. 3 is for the imaginary part ϵ_i . The curves are designated as follows: solid line for sample S_1 , dot-dashed for sample S_2 and dotted for sample S_3 . In Table 2 we give their values at 11.424 GHz to indicate the deviation is about a few percent for ϵ_r , whereas the fluctuation can be several times larger for ϵ_i . These measured data will be used in subsequent 3D calculations.

Table II
Complex dielectric constants of three ceramic samples at 11.424 GHz.

Sample	ϵ_r	ϵ_i
S_1	25.0	8.62
S_2	25.8	9.35
S_3	25.0	9.40

IV. LOAD DESIGN

In the load geometry depicted in Fig. 1, the ceramic wedge consists of a front taper transitioning to a constant thickness for the rest of its length. Hence, there are three dimensions to be determined: the total length L , the thickness h , and the taper length s . The last two control the angle of the taper. We will use a 2D analysis to determine L and h approximately.

In the uniform portion of the load, the cross section is that of a rectangular guide filled at each narrow wall with a dielectric of thickness h . If one assumes the end wall of the load is far away, then this simple geometry can be solved readily by mode-matching techniques to give the complex propagation constant

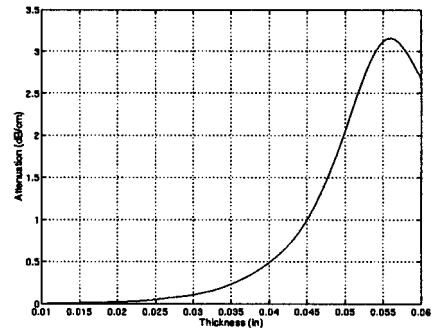


Figure 4. Attenuation rate in dB/cm versus ceramic thickness in inches.

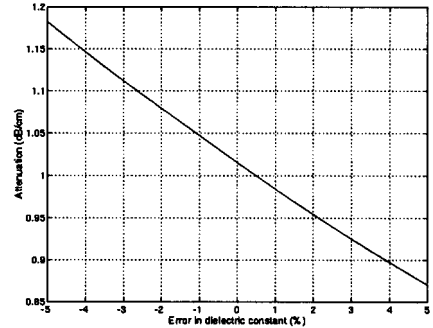


Figure 5. Sensitivity of attenuation rate in dB/cm to fluctuation in ϵ_i in %.

β for a wave traveling down the load. The attenuation rate in dB per centimeter is obtained from the imaginary part of β , and Fig. 4 shows how it depends on h for the mean value of ϵ taken from the three samples in Table 2. It rises slowly at small h , then increases rapidly starting around .045 in to reach a peak near .055 in, and falls off beyond. In Fig. 5 we show the sensitivity of the attenuation rate to variation in ϵ_i in percent assuming $h = .045$ in. A fluctuation of 5% in ϵ_i results in a 15% change in attenuation per centimeter.

In order to dissipate the power gradually to avoid excessively high temperature rise, we opted for 1 dB attenuation per centimeter and fixed h to be .045 in. Then L is chosen to be 10 in for a reasonable length and adequate attenuation, greater than 40 dB. The actual performance of the load has to include the taper whose length s we have yet to determine; this requires modeling the real geometry with the 3D MAFIA code [3].

V. MAFIA SIMULATION

Time-domain S-parameter simulations have been carried out for the load geometry of Fig. 1. An incident TE_{10} mode at a specified frequency propagates down a short section of empty guide towards the load and from its reflection at steady-state, the VSWR can be calculated. At the same time, the electric fields at time intervals a quarter period apart are used to find the power dissipation in the lossy ceramic. Then the peak power density is located and is normalized to 3 kW input power to obtain the correct value. The dielectric properties of the ceramic at the simulated frequency is read off the data shown in Figs. 2 and 3 for the appropriate sample used.

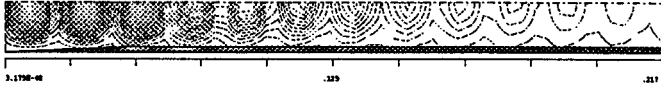


Figure 6. Time-average energy density in the load.

Fig. 6 shows the top view of one half of the load looking down on the broad side of the guide, and the thin ceramic wedge can be seen at the bottom along the narrow wall. The time-average energy density contours are displayed, showing the RF power incident from the left and diminishing in intensity as it propagates to the right into the load. This picture demonstrates vividly how the load works. The incident TE_{10} wave undergoes mode conversion as it encounters the dielectric in the load. The new mode splits its field between the empty guide and the dielectric. The portion inside the dielectric is attenuated (at a rate close to that predicted by the 2D analysis), and is responsible for the power absorption.

The effectiveness of the load depends on how well the incoming power is channeled into the dielectric and how gradually this power transfer can be achieved. It is evident that the optimum is when the power is incident near the grazing angle because this offers the largest surface. Below the grazing angle, the power glances off the dielectric and reflects back from the end wall. Above it, the power penetrates the dielectric over a small area, leading to high dissipation density. Fig. 7 shows a region of power dissipation near the end of the taper. This is the optimal case where the power is spread out over several wavelengths.

VI. LOAD PERFORMANCE

We have evaluated different designs and the results for the final design are summarized in Table 3. It has a taper angle of 1.7 degrees that corresponds to a taper length s of 1.5 in. All three samples were simulated at 11.424 GHz. Sample S_3 was also studied at two other frequencies to determine if the load meets the bandwidth requirement. The peak temperature T_{max} in $^{\circ}C$ is calculated from

$$T_{max} = \frac{Qh^2}{2k_{AlN}} \left\{ 1 + \frac{2dk_{AlN}}{hk_{Cu}} \right\} \quad (1)$$

where Q is the peak power density from MAFIA in W/cm^3 , h is the ceramic thickness as before, d is the distance from the ceramic to the cooling water, and k_{AlN} , k_{Cu} are the thermal conductivity of the ceramic and copper respectively. This 1D model is valid because the variation in the third dimension in Fig. 7 is negligible since the TE_{10} mode is uniform in this direction. It is apparent from Eq. (1) that T_{max} can be kept low by having the peak power density not be excessively high, by making the ceramic as thin as possible, and by moving the cooling water as close to the ceramic as practically possible.

The load performance given in Table 3 indicates that the design has a good match and reasonable temperature rise in the frequency range of interest. We note that the performance may be slightly worse when the ceramic strip is brazed on in the form of buttons.

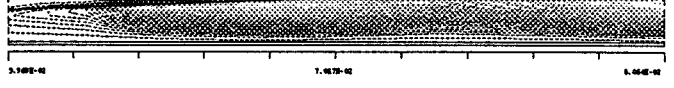


Figure 7. Power dissipation density in the load.

Table III

Load performance using different ceramic samples.

Sample	Frequency (GHz)	VSWR	T_{max} ($^{\circ}C$)
S_3	11.000	1.094	146
	11.424	1.056	132
	11.800	1.038	115
S_1	11.424	1.070	147
S_2	11.424	1.042	156

VII. CONCLUSION

We have presented a dry load design whose performance satisfies the requirements for the NLCTA application. It comprises two tapered strips of AlN + 7% glassy carbon ceramic, 0.045 in thick and 10 in long. To avoid differential expansion problems between the copper waveguide walls and the ceramic, the strips are broken up into 0.35 in square buttons, which are brazed onto the narrow side walls of WR90 waveguide. Such a load is presently being fabricated for high power test.

References

- [1] W.R. Fowkes *et al.*, High Power RF Window and Waveguide Component Development and Testing Above 100 MW at X-Band, SLAC PUB 5877, Stanford Linear Accelerator Center, Aug. 1992.
- [2] I.E. Campisi *et al.*, The Design and Production of the High-Order-Mode Loads for CEBAF, Proceedings of the 1993 Particle Accelerator Conference, p.1220-1222.
- [3] The MAFIA collaboration, *User's Guide MAFIA Version 3.2*, CST GmbH, Luteschlägerstr.38, D6100 Darmstadt.